

Control of Outmost Poloidal Flux Surface of Tokamak Plasma in RTP

Kwang Won Lee and Byung Hoon Oh

Korea Atomic Energy Research Institute

(Received September 24, 1992)

RTP에서 토카막 플라즈마의 폴로이달 등자속면 제어

이광원 · 오병훈

한국원자력연구소

(1992. 9. 24 접수)

Abstract

The paper describes : i) Mathematical modeling of poloidal flux to define and calculate the tokamak plasma position based on a property of the plasma boundary which is always a flux surface. Controlling the plasma boundary position is therefore equivalent to equalizing the flux value on several points belonging to a curve tangent to the limiter. ii) Experimental method for determining the outmost poloidal isoflux surface by a linear combination of measurements of magnetic fluxes, fields and field gradients, without requiring knowledge of internal plasma parameters for the feedback control, i.e., with neither corrections for variation in the poloidal beta and the plasma current distribution, nor compensations for the induced currents in the vacuum vessel. iii) Feedback control algorithm for the regulation of plasma boundary position and its electronics hardware based on the PID control theory. iv) Experimental results obtained from the RTP tokamak experiments using the present plasma control system.

요 약

본 논문은 다음의 내용을 기술한다 : i) 토카막 플라즈마의 경계면을 정의하고 계산하는 폴로이달 자속의 수학적 모형을 플라즈마경계면과 등자속면이 일치한다는 사실로부터 수립한다. 따라서 플라즈마의 경계위치를 제어한다 함은 리미터 접선상의 여러 점들에서 자속값을 같게 만드는 것을 의미한다. ii) 자속, 자장, 자장구배의 선형조합으로 최외각 폴로이달 등자속면을 측정하는 방법을 제시한다. 이 방법은 내부플라즈마변수를 알 필요가 없어서 폴로이달베타와 플라즈마전류분포의 변동에 따르는 수정이나 진공용기의 유도전류를 보상하지 않아도 된다. iii) 플라즈마의 경계면 위치조정을 위한 폐환제어 알고리즘을 수립하고, PID 제어이론을 기초로 해당 전자장비를 제작한다. iv) 본 플라즈마 제어계를 사용한 RTP토카막 실험의 결과를 논의한다.

1. Introduction

In a tokamak plasma, the interaction between high temperature plasma and limiter causes the remarkable influx of impurities and successive disruptive instability. Therefore, it becomes important to maintain the plasma in the optimum position to have a tokamak plasma of high density and temperature. In order to maintain a plasma column in the geometrical center of its vacuum vessel, the externally applied equilibrium magnetic field must be adjusted according to the changes in the plasma parameters such as the plasma current and poloidal beta. Furthermore, from the point of view of tokamak plasma engineering, a precise regulation of plasma position can extend the plasma duration and improve the operational efficiency of pulsed experiment for a given tokamak.

The plasma position in tokamaks is usually determined with magnetic probes. In existing facilities, however, the position signals defined as current center depend not only on the plasma position but also on the poloidal beta and the internal inductance of plasma. In practice, difficulties are encountered in measuring the internal plasma parameters and including them quickly enough in calculation to regulate the plasma position. It is even more difficult to take the time dependent inductive current in vessel into account which also influences greatly the poloidal field. To obviate all these difficulties, a new position measuring method and control algorithm are to be developed based on the outmost poloidal flux surface control.

The RTP tokamak ($R=0.72$ m, $a=0.175$ m), which is the refurbished Petula tokamak previously operated at Grenoble, France, from 1982 to 1986, is presently being commissioned at the FOM-Institute for plasma physics 'Rijnhuizen', Nederland, in which the main theme of fusion research is the study of transport mechanism of tokamak plasma [1]. More concretely, the ex-

perimental work will focus on determining the radial and poloidal structure of plasma equilibrium as accurately as possible. For this research program a fine control of plasma position is recommended. The selected machine parameters of RTP are given in Table 1.

RTP has two bar limiters positioned symmetrically at the top and the bottom so that the plasma boundary is referenced vertically, and it was operated by the current centre position control scheme concerning plasma control. With the existing control system, it was difficult to have a reliable breakdown and build up of the plasma current due to the abnormally high liner current.

The new position feedback control system comprises a PID(Proportional-Integral-Differential) controller providing the control signals which are transmitted to the chopper controlled power supplies of the equilibrium field coils and a flux calculator which calculates the poloidal flux differences between symmetric top and bottom reference positions and between the desired inboard and outboard boundaries of the plasma from the measurements by magnetic field pick-up probes and saddle loops. This method of controlling the position of magnetic surfaces has been previously applied with success in ASDEX[2], JET[3], and also in other tokamak machines. In RTP, flux feedback is enabled even before the onset of the plasma current to achieve a highly reliable breakdown and build-up of the plasma current. The plasma position during the gas injection can also

Table 1. Selected Machine Parameters of RTP Tokamak

Major radius of plasma	0.72 m
Minor radius of plasma	0.175 m
Toroidal magnetic field at minor axis	2.2 T
Plasma current	100 kA
Plasma duration(Flat top)	120 ms

be regulated by introducing an integral and a differential action into the controller.

2. Poloidal Flux at the Plasma Boundary

To determine the poloidal flux at the plasma surface, we will use the following scheme of

$$\psi(\rho_p, \theta) = \psi(\rho_M, \theta) + 2\pi \int_{\rho_M}^{\rho_p} (R + \rho \cos\theta) B_\theta(\rho, \theta) d\rho \quad (1)$$

for a given θ -direction in which ρ_p and ρ_M are the radial positions of limiter and saddle loop, respectively. The position variables are referred to Fig.1 and poloidal flux is defined as in Fig.2.

Assuming that the flux value at a certain point can be calculated by a second order expansion of the flux measured, $B_\theta(\rho, \theta)$ can be represented as a linear function of ρ around ρ_b ;

$$B_\theta(\rho, \theta) \equiv B_\theta(\rho_b, \theta) + (\rho - \rho_b) \left. \frac{\partial B_\theta}{\partial \rho} \right]_{\rho=\rho_b} \quad (2)$$

where ρ_b indicates the position of a poloidal field pick-up probe. Then,

$$\psi(\rho_p, \theta) \equiv \psi(\rho_M, \theta) - a_\theta B_\theta(\rho_b, \theta) - b_\theta \left. \frac{\partial B_\theta}{\partial \rho} \right]_{\rho=\rho_b} \quad (3)$$

where

$$a_\theta = 4\pi c_\theta \{R + (\rho_M - c_\theta) \cos\theta\}$$

$$b_\theta = 4\pi c_\theta \{R(h - c_\theta) + (h\rho_M - (\rho_M + h)c_\theta + 4/3 c_\theta^2) \cos\theta\}$$

$$c_\theta = (\rho_M - \rho_p) / 2 = d_\theta / 2,$$

$$h = \rho_M - \rho_b$$

Here, $\Psi(\rho_M, \theta)$ and $B_\theta(\rho_b, \theta)$ can be determined by measuring the signals from a set of saddle loops and B_θ pick up coils installed as in Fig.1. And also radial gradient of B_θ will be obtained with a formula deduced from $\nabla \times \mathbf{B} = \mu_0 \{ \mathbf{J} + \epsilon_0 (\partial \mathbf{E} / \partial t) \}$, i.e.,

$$\frac{\partial B_\theta}{\partial \rho} = \left(\frac{\partial B_\rho}{\partial \theta} - B_\theta \right) \frac{1}{\rho} + \mu_0 (J_\phi + \epsilon_0 \frac{\partial E_\phi}{\partial t}) \quad (4)$$

in which $\frac{\partial B_\rho}{\partial \theta}$ can be measured by B_ρ pick up coils or saddle loops approximately, and J_ϕ and

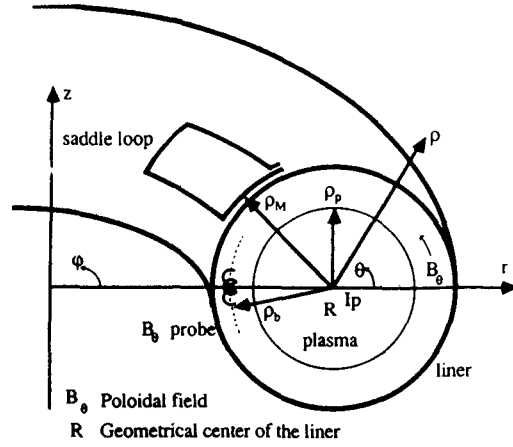


Fig. 1. Toroidal Coordinate System and Characteristic Position Variables.

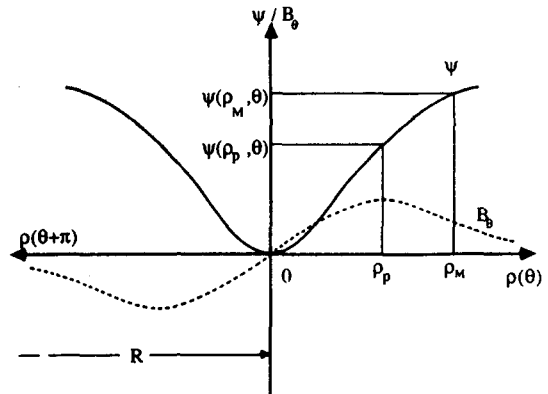


Fig. 2. Poloidal Field and Its Flux Function

$\frac{\partial E_\phi}{\partial t}$ are from the liner current distribution and the toroidal loop voltages respectively. Substituting eq.(4) into eq.(3) and deriving the flux difference between θ_i and θ_j -poloidal directions, one obtains

$$\begin{aligned} \delta\psi_{ij} = \psi_{pi} - \psi_{pj} = & (\psi_{Mi} - \psi_{Mj}) - (A_i B_{\theta i} - A_j B_{\theta j}) \\ & + (C_i \frac{\partial B_{\rho i}}{\partial \theta} - C_j \frac{\partial B_{\rho j}}{\partial \theta}) - \mu_0 (b_i J_{\phi i} - b_j J_{\phi j}) \\ & - \frac{1}{c^2} \frac{\partial}{\partial t} (b_i E_{\phi i} - b_j E_{\phi j}) \end{aligned} \quad (5)$$

Here some abbreviated notations are used for convenience;

$$\Psi_{pi} = \Psi(\rho_p, \theta_i)$$

$$\Psi_{Mi} = \Psi(\rho_M, \theta_i)$$

$$B_{\theta i} = B_{\theta}(\rho_b, \theta_i)$$

$$B_{\rho i} = B_{\rho}(\rho_b, \theta_i)$$

$$J_{\phi i} = J_{\phi}(\rho_b, \theta_i)$$

$$E_{\phi i} = E_{\phi}(\rho_b, \theta_i)$$

$$a_i = a_{\theta i}$$

$$b_i = b_{\theta i} \equiv 4\pi\epsilon_i(h - c_i)(R + \rho_M \cos\theta_i)$$

and,

$$A_i = a_i - (b_i/\rho_b), \quad C_i = - (b_i/\rho_b)$$

Last two terms of eq.(5) can be deduced from the liner current and the toroidal loop voltage difference between the inboard and outboard positions of plasma column, which are important in the transient stage such as breakdown, plasma current build up phase and/or disruption but not important in the steady state of the well controlled plasma. So, last two terms are to be neglected hereafter. These may be considered later by applying some compensation terms to be determined experimentally with the formulation of $I_{\text{liner}} + \tau \frac{\partial}{\partial t} (\Psi_{\theta=180^\circ} - \Psi_{\theta=0^\circ})$ if needed. $\delta\Psi_{ij}$ will be used as a feedback error quantity for the plasma position control. The plasma boundary is always the outmost flux surface in equilibrium. So, controlling the plasma boundary is to equalize the flux value on it.

The important flux difference quantities for the tokamak operation and the study of the poloidal structure of plasma are ;

- (i) Vertical flux difference between $\theta_i=0$ and $\theta_i=\pi$ for horizontal position control ;

$$\begin{aligned} \delta\Psi_V = \Psi_{p(0)} - \Psi_{p(\pi)} &= (\Psi_{M(0)} - \Psi_{M(\pi)}) \\ &- (A_0 B_{\theta(0)} - A_{\pi} B_{\theta(\pi)}) + (C_0 \frac{\partial B_{\rho(0)}}{\partial \theta} - C_{\pi} \frac{\partial B_{\rho(\pi)}}{\partial \theta}) \end{aligned} \quad (6)$$

- (ii) Radial flux difference between $\theta_i=\pi/2$, and $\theta_i=3\pi/2$ for vertical position control ;

$$\begin{aligned} \delta\Psi_R = \Psi_{p(\pi/2)} - \Psi_{p(3\pi/2)} &= (\Psi_{M(\pi/2)} - \Psi_{M(3\pi/2)}) \\ &- (A_{\pi/2} B_{\theta(\pi/2)} - A_{3\pi/2} B_{\theta(3\pi/2)}) + (C_{\pi/2} \frac{\partial B_{\rho(\pi/2)}}{\partial \theta} - C_{3\pi/2} \frac{\partial B_{\rho(3\pi/2)}}{\partial \theta}) \end{aligned} \quad (7)$$

- (iii) Quarter flux differences to estimate the eccentricity of plasma cross section ;

$$\begin{aligned} \delta\Psi_1 = \Psi_{p(\pi/2)} - \Psi_{p(0)} &= (\Psi_{M(\pi/2)} - \Psi_{M(0)}) - (A_{\pi/2} B_{\theta(\pi/2)} \\ &- A_0 B_{\theta(0)}) + (C_{\pi/2} \frac{\partial B_{\rho(\pi/2)}}{\partial \theta} - C_0 \frac{\partial B_{\rho(0)}}{\partial \theta}) \end{aligned} \quad (8)$$

$$\begin{aligned} \delta\Psi_4 = \Psi_{p(3\pi/2)} - \Psi_{p(0)} &= (\Psi_{M(3\pi/2)} - \Psi_{M(0)}) - (A_{3\pi/2} B_{\theta(3\pi/2)} \\ &- A_0 B_{\theta(0)}) + (C_{3\pi/2} \frac{\partial B_{\rho(3\pi/2)}}{\partial \theta} - C_0 \frac{\partial B_{\rho(0)}}{\partial \theta}) \end{aligned} \quad (9)$$

$$\begin{aligned} \delta\Psi_2 = \Psi_{p(\pi/2)} - \Psi_{p(\pi)} &= (\Psi_{M(\pi/2)} - \Psi_{M(\pi)}) - (A_{\pi/2} B_{\theta(\pi/2)} \\ &- A_{\pi} B_{\theta(\pi)}) + (C_{\pi/2} \frac{\partial B_{\rho(\pi/2)}}{\partial \theta} - C_{\pi} \frac{\partial B_{\rho(\pi)}}{\partial \theta}) \end{aligned} \quad (10)$$

$$\begin{aligned} \delta\Psi_3 = \Psi_{p(3\pi/2)} - \Psi_{p(\pi)} &= (\Psi_{M(3\pi/2)} - \Psi_{M(\pi)}) - (A_{3\pi/2} B_{\theta(3\pi/2)} \\ &- A_{\pi} B_{\theta(\pi)}) + (C_{3\pi/2} \frac{\partial B_{\rho(3\pi/2)}}{\partial \theta} - C_{\pi} \frac{\partial B_{\rho(\pi)}}{\partial \theta}) \end{aligned} \quad (11)$$

In RTP, B_{ρ} pick up coils give positive $B_{\theta i}$'s values for the poloidal field with positive θ -direction and a set of saddle loops can give Ψ_{Mij} and $\frac{\partial B_{\rho i}}{\partial \theta}$. B_{ρ} pick-up coils can also give $\frac{\partial B_{\rho i}}{\partial \theta}$ even more accurately. However, the signals of each B_{ρ} are not available separately in RTP.

3. Magnetic Measurement

RTP has 12 saddle loops with the toroidal span of $\Delta\varphi = \pi/10$ and the equipartitional poloidal angle span of $\Delta\varphi = \pi/6$. Flux through each saddle loop $\phi_{\theta i}^s$ is given by $\phi_{\theta i}^s = T_c u_{\theta i}^s$, ($\theta = 0^\circ, 30^\circ, 60^\circ, \dots, 330^\circ$) in which $u_{\theta i}^s$ is the output signal of dedicated integrator of each saddle coil and T_c is

its integrating time constant. $\phi_{\theta_i}^s$ has positive sign for the outward flux from the inside of vacuum vessel. Defining the quarter poloidal fluxes through the torus surface of $\rho = \rho_M$ as ;

$$\begin{aligned}\phi_1 &= 20(1/2\phi_{0^\circ}^s + \phi_{30^\circ}^s + \phi_{60^\circ}^s + 1/2\phi_{90^\circ}^s) \\ \phi_2 &= 20(1/2\phi_{90^\circ}^s + \phi_{120^\circ}^s + \phi_{150^\circ}^s + 1/2\phi_{180^\circ}^s) \\ \phi_3 &= 20(1/2\phi_{180^\circ}^s + \phi_{210^\circ}^s + \phi_{240^\circ}^s + 1/2\phi_{270^\circ}^s) \\ \phi_4 &= 20(1/2\phi_{270^\circ}^s + \phi_{300^\circ}^s + \phi_{330^\circ}^s + 1/2\phi_{0^\circ}^s)\end{aligned}$$

then,

$$\begin{aligned}\delta\psi_{MV} &= \psi_{M(0)} - \psi_{M(\pi)} = \phi_1 + \phi_2 = -(\phi_3 + \phi_4) \\ \delta\psi_{MR} &= \psi_{M(\pi/2)} - \psi_{M(3\pi/2)} = \phi_2 + \phi_3 = -(\phi_1 + \phi_4) \\ \delta\psi_{M1} &= \psi_{M(\pi/2)} - \psi_{M(0)} = -\phi_1 \\ \delta\psi_{M2} &= \psi_{M(\pi/2)} - \psi_{M(\pi)} = \phi_2 \\ \delta\psi_{M3} &= \psi_{M(3\pi/2)} - \psi_{M(\pi)} = -\phi_3 \\ \delta\psi_{M4} &= \psi_{M(3\pi/2)} - \psi_{M(0)} = \phi_4\end{aligned}$$

And with $B_{\theta_i}^s = \phi_{\theta_i}^s / A_{\theta_i}^s$ ($A_{\theta_i}^s =$ surface area of θ_i -saddle loop), $\frac{\partial B_{\rho_i}}{\partial \theta}$ can also be calculated as following.

$$\begin{aligned}\frac{\partial B_{\rho(0)}}{\partial \theta} &= (3/\pi)(B_{30^\circ}^s - B_{330^\circ}^s), \\ \frac{\partial B_{\rho(\pi/2)}}{\partial \theta} &= (3/\pi)(B_{120^\circ}^s - B_{60^\circ}^s) \\ \frac{\partial B_{\rho(\pi)}}{\partial \theta} &= (3/\pi)(B_{210^\circ}^s - B_{150^\circ}^s), \\ \frac{\partial B_{\rho(3\pi/2)}}{\partial \theta} &= (3/\pi)(B_{300^\circ}^s - B_{240^\circ}^s)\end{aligned}$$

The A_i 's and C_i 's given by $A_i = a_i - b_i / \rho_b = a_i + C_i$, and $C_i = -(b_i / \rho_b)$ can be determined from the geometrical factor,

$$\begin{aligned}C_i &= \frac{4\pi e_i}{\rho_b} \{ R(e_i - h) - (h\rho_M - (\rho_M + h)e_i + 4/3 e_i^2) \cos\theta \} \\ &\equiv \frac{4\pi e_i}{\rho_b} (e_i - h)(R + \rho_M \cos\theta)\end{aligned}$$

$$A_i = 4\pi e_i \{ R + (\rho_M - e_i) \cos\theta \} + C_i$$

In RTP, $R=0.72$ m ; $\rho_M=0.24$ m ; $\rho_b=0.213$ m ; $h=0.027$ m, and the desired cross sectional shape

of the plasma is circular i.e., all e_i 's or ρ_{pi} 's have the same value of e or ρ_p respectively ($e_i=e$, $\rho_{pi}=\rho_p$, $i=0, \pi/2, \pi, 3\pi/2$). So, the constants A_i 's and C_i 's can be determined numerically for each plasma diameter. Then eqs.(6)~(11) become ;

$$\begin{aligned}\delta\psi_V &= (\phi_1 + \phi_2) - (A_0 B_{\theta(0)} - A_\pi B_{\theta(\pi)}) \\ &\quad + \frac{3}{\pi} \{ C_0 (B_{30^\circ}^s - B_{330^\circ}^s) - C_\pi (B_{210^\circ}^s - B_{150^\circ}^s) \}\end{aligned}$$

$$\begin{aligned}\delta\psi_R &= (\phi_2 + \phi_3) - (A_{\pi/2} B_{\theta(\pi/2)} - A_{3\pi/2} B_{\theta(3\pi/2)}) \\ &\quad + \frac{3}{\pi} \{ C_{\pi/2} (B_{120^\circ}^s - B_{60^\circ}^s) - C_{3\pi/2} (B_{300^\circ}^s - B_{240^\circ}^s) \}\end{aligned}$$

$$\begin{aligned}\delta\psi_1 &= -\phi_1 - (A_{\pi/2} B_{\theta(\pi/2)} - A_0 B_{\theta(0)}) \\ &\quad + \frac{3}{\pi} \{ C_{\pi/2} (B_{120^\circ}^s - B_{60^\circ}^s) - C_0 (B_{30^\circ}^s - B_{330^\circ}^s) \}\end{aligned}$$

$$\begin{aligned}\delta\psi_2 &= \phi_2 - (A_{\pi/2} B_{\theta(\pi/2)} - A_\pi B_{\theta(\pi)}) \\ &\quad + \frac{3}{\pi} \{ C_{\pi/2} (B_{120^\circ}^s - B_{60^\circ}^s) - C_\pi (B_{210^\circ}^s - B_{150^\circ}^s) \}\end{aligned}$$

$$\begin{aligned}\delta\psi_3 &= -\phi_3 - (A_{3\pi/2} B_{\theta(3\pi/2)} - A_\pi B_{\theta(\pi)}) \\ &\quad + \frac{3}{\pi} \{ C_{3\pi/2} (B_{300^\circ}^s - B_{240^\circ}^s) - C_\pi (B_{210^\circ}^s - B_{150^\circ}^s) \}\end{aligned}$$

$$\begin{aligned}\delta\psi_4 &= \phi_4 - (A_{3\pi/2} B_{\theta(3\pi/2)} - A_0 B_{\theta(0)}) \\ &\quad + \frac{3}{\pi} \{ C_{3\pi/2} (B_{300^\circ}^s - B_{240^\circ}^s) - C_0 (B_{30^\circ}^s - B_{330^\circ}^s) \}\end{aligned}$$

In the saddle flux measurement, we have had the error such as $\sum \phi_{\theta_i}^s = \delta \phi$. So, $\phi_{\theta_i}^s$ is to be compensated so as to $\sum (\phi_{\theta_i}^s + \delta \phi_{\theta_i}^s) = 0$, or $\sum \delta \phi_{\theta_i}^s = -\delta \phi$ according to the flux conservation. It would be helpful to eliminate or reduce such a kind of measured flux error if the saddle loop is made of a electrostatically shielded cable instead of a single cable presently being used. Now, if we assume that $\delta \phi_{\theta_i}^s = -(\delta \phi / 12)$ and $\delta \phi_i = -(\delta \phi / 4)$, [$i=1,2,3,4$] to meet the flux conservation, the compensated saddle fluxes are to be defined newly as following ;

$$\begin{aligned}(\phi_1 + \phi_2) &\rightarrow (\phi_1 + \phi_2) - \delta\phi/2 = (\phi_1 + \phi_2 - \phi_3 - \phi_4)/2 \\ (\phi_2 + \phi_3) &\rightarrow (\phi_2 + \phi_3) - \delta\phi/2 = (-\phi_1 + \phi_2 + \phi_3 - \phi_4)/2 \\ \phi_i &\rightarrow \phi_i - \delta\phi/4, \quad (i = 1, 2, 3, 4)\end{aligned}$$

With these, the vertical and the radial flux differences at the plasma boundary can be rewritten as ;

$$\begin{aligned} \delta\psi_V = 10 \{ & (1 + \frac{0.3C_0}{\pi A^s_{30'}}) \phi^{s_{30'}} + \phi^{s_{60'}} + \phi^{s_{90'}} + \phi^{s_{120'}} \\ & + (1 + \frac{0.3C_\pi}{\pi A^s_{150'}}) \phi^{s_{150'}} - (1 + \frac{0.3C_\pi}{\pi A^s_{210'}}) \phi^{s_{210'}} - \phi^{s_{240'}} \\ & - \phi^{s_{270'}} - \phi^{s_{300'}} - (1 + \frac{0.3C_0}{\pi A^s_{330'}}) \phi^{s_{330'}} \} \\ & - (A_0 B_{\theta(0)} - A_\pi B_{\theta(\pi)}) \end{aligned} \quad (12)$$

$$\begin{aligned} \delta\psi_R = 10 \{ & (1 + \frac{0.3C_{\pi/2}}{\pi A^s_{120'}}) \phi^{s_{120'}} + \phi^{s_{150'}} + \phi^{s_{180'}} + \phi^{s_{210'}} \\ & + (1 + \frac{0.3C_{3\pi/2}}{\pi A^s_{240'}}) \phi^{s_{240'}} - (1 + \frac{0.3C_{3\pi/2}}{\pi A^s_{300'}}) \phi^{s_{300'}} \\ & - \phi^{s_{330'}} - \phi^{s_{0'}} - \phi^{s_{30'}} - (1 + \frac{0.3C_{\pi/2}}{\pi A^s_{60'}}) \phi^{s_{60'}} \} \\ & - (A_{\pi/2} B_{\theta(\pi/2)} - A_{3\pi/2} B_{\theta(3\pi/2)}) \end{aligned} \quad (13)$$

The terms of these equations are all measurable via saddle loops and B_θ magnetic pickup probes.

4. Plasma Position Displacement

On the isoflux surface, the poloidal flux function

satisfies $\delta\Psi_{Mij}=0$. The plasma position displacement at θ_j can be defined as Δe_j , which satisfies the equation of

$$\Psi_{pi}(e_i) - \Psi_{pj}(e_j = e_i + \Delta e_j) = 0 \quad (14)$$

for a referenced plasma boundary position ρ_{pi} . From eq.(5) and eq.(14), Δe_j is

$$\Delta e_j = \frac{-\delta\Psi_{ij}(e_i = e_j = e)}{4\pi(U_j B_{\theta j} - V_j \frac{\partial B_{\theta j}}{\partial \theta})} \quad (15)$$

where

$$U_j = R(2 - \rho_p/\rho_b) + \rho_M(1 + \rho_p/\rho_M - \rho_p/\rho_b) \cos\theta_j$$

$$V_j = (1 - \rho_p/\rho_b)(R + \rho_M \cos\theta_j)$$

in the region of $(\Delta e_j/\rho_b) \ll 1$. Of these, vertical displacement Δe_L and horizontal displacement Δe_L are for the cases of $[i=\pi/2, j=3\pi/2]$ and $[i=0, j=\pi]$ respectively.

5. Feedback Control Loop

Non-zero poloidal flux errors of eqs.(12) and (13) are used as feedback signals in operating the power supplies for the vertical and the horizontal field coils, respectively.

5.1. Horizontal Position Control

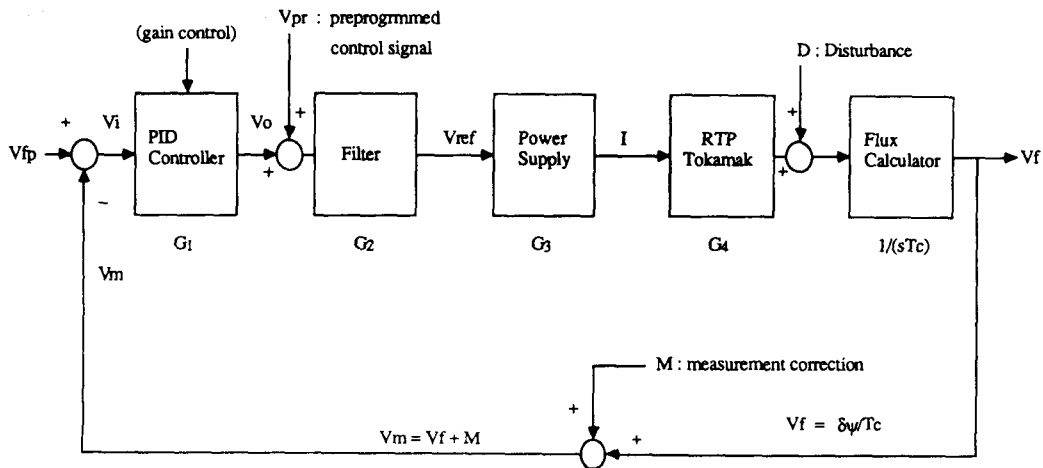


Fig. 3. Block Diagram Describing the Scheme of Feedback Loop for the Plasma Boundary Control of RTP

A block diagram of the horizontal position control system is shown in Fig.3. Power supply of VF coil is operated by chopping switch in a mode where the output current into V.F.-coil is essentially proportional to the control voltage V_{ref} via the internal feedback loop. We assume that the frequency of chopped output voltage of capacitor bank, and consequently the changing rate of the coil current I is much faster than that of vertical flux difference $\delta\Psi$ corresponding to the plasma position oscillation and/or drift. The appropriate controller is therefore a proportional controller. The addition of derivative and integral feedback permits an increase of the loop gain without causing overshoot and poorly damped oscillatory behavior of the response upon perturbations in both fast and slow phase. The controller gain can be varied between 0 and 2.2 by a potentiometer setting. V_{fp} is the input for the modulation of the flux difference signal and consequently of the plasma boundary. V_{pr} is the (pre)programmed control voltage input, which is used not only to assist feedback loop during phases of rapid changes such as fast rising of plasma current but also to provide a bias field. It might be proportional to the plasma current ($V_{pr} \sim I_p$) as a feed-forward term to reduce the responsibility of feedback loop. M is the input port prepared to correct the flux measurement error. The block G_2 is an RC-filter for cutting off high frequency noise on the signal line produced by the plasma and the derivative element.

A simplified model yields the following transfer functions for each block of Fig.3 ;

$$G_1 = K_p \left(1 + \frac{K_i}{\eta + T_i s} + \frac{K_d T_d s}{1 + T_u s} \right)$$

$$G_2 = \frac{1}{1 + T_f s}$$

$$G_3 = \frac{K_1}{1 + T_1 s}$$

$$G_4 = \frac{K_2}{1 + T_2 s}$$

in which

K_p = controller gain (0~2.2)

K_i = gain factor of integral action (0~1)

K_d = gain factor of differential action (0~1)

$K_1 = I/V_{ref}$: control sensitivity of power supply (200 A/V)

K_2 = flux change for 1A current of VF coil, depending on the chosen number of turns of V.F.- coil and, to some extent, on plasma parameter. $K_2 \sim 4.8 \times 10^{-5}$ (Vs/A) without plasma.

T_C = effective integration time constant in magnetic flux measurement (22 ms)

T_i = integral time constant of the PID controller (3.9 ms)

T_d = derivative time constant of the PID controller (11 ms)

T_u = delay time due to the derivative feedback electronics (0.11 ms)

T_f = RC time constant of the passive filter (5 ms)

T_1 = response time of the power supply (~1 ms), depending on the charging voltage of capacitor bank and the crowbar resistance [4]

T_2 = vessel tranverse field penetration time (2 ms)

η^{-1} = gain of the integral feedback electronics

From a simplified analysis on the feedback loop of Fig.3, one finds the following response relations.

$$V_f = \frac{G}{1+G} V_{fp} - \frac{G}{1+G} M + \frac{G}{G_1(1+G)} V_{pr} + \frac{1}{1+G} \frac{\partial D}{\partial t}$$

$$V_m = \frac{G}{1+G} V_{fp} + \frac{1}{1+G} M + \frac{G}{G_1(1+G)} V_{pr} + \frac{1}{1+G} \frac{\partial D}{\partial t}$$

$$V_i = \frac{1}{1+G} \left(V_{fp} - M - \frac{\partial D}{\partial t} \right) - \frac{G}{G_1(1+G)} V_{pr} \\ = \frac{1}{G} \left(V_f - \frac{\partial D}{\partial t} \right) - \frac{1}{G_1} V_{pr}$$

where

$$\frac{\partial D}{\partial t} = \frac{D}{T_C}$$

$$G = \frac{G_1 G_2 G_3 G_4}{T_C} = \frac{(K_p K_1 K_2 / T_C) \{ (\eta + T_1 s)(1 + (T_u + T_D) s) + K_i (1 + T_u s) \}}{(1 + T_1 s)(1 + T_2 s)(1 + T_3 s)(1 + T_u s)(\eta + T_1 s)}$$

Characteristic equation of the above response functions has five poles. By the Ziegler–Nichols method, the optimal values of PID controller constants are determined as ; $K=0.38$, $T_I=6$ ms, $T_D=1.5$ ms, in which $K=K_0 K_p$, $K_0=K_1 K_2 / T_C$, $T_I=T_i / K_i$, $T_D=T_d K_d$ and one assumes that $\eta \sim 0$, $T_u \sim 0$.

5.2. Vertical Position Control

The feedback scheme of the vertical position control i.e., radial field control loop is almost same in principle as that of horizontal position feedback control. Some minor changes in gain factor and time constants of each devices are ; $K_p=0 \sim 5.0$, $K_1=140$ A/V, $K_2=1.1 \times 10^{-5}$ Vs/A, $T_C=10.8$ ms, $T_u=0.05$ ms, $T_I \sim 1.5$ ms, and the normal settings become $K=0.31$, $T_I=10$ ms, $T_D=2.5$ ms.

6. Experimental Results

For the purpose of feedback control, the vertical flux difference $\delta \Psi_V$ of eq.(12) is processed to the flux error signal $V_{f,V}$ i.e., $V_{f,V} = \delta \Psi_V / T_{C,V}$, and $\delta \Psi_R$ of eq.(13) is to $V_{f,R}$ i.e., $V_{f,R} = \delta \Psi_R / T_{C,R}$ in flux calculator. Additive subscript $_V$ indicates the variable relevant to the vertical field(horizontal position) control and $_R$ the radial field(vertical position) control. $V_{pr,V}$ and $V_{pr,R}$ are empirically determined as $V_{pr,V}[\text{V}] = 0.03 I_p [\text{kA}]$ and $V_{pr,R} = 1.3[\text{V}]$ in RTP experiment. Of these, $V_{pr,V}$ can also be determined analytically[5]. The values of these terms are not so critical in accuracy but essential to improve the control performance since it can greatly reduce the responsibility of feedback loop. So, $V_{ref,V}$ comprises a flux feedback term($V_{f,V}$ through PID controller) and a term $V_{pr,V}$ proportional to the plasma current approximately equal to $\frac{\rho_{pl}}{4\pi R} (\ln \frac{8R}{\rho_n} + \beta_p + \frac{1-3}{2})$ but neglecting the

variations of internal plasma parameters β_p and I_p . $V_{ref,R}$ comprises a flux feedback term($V_{f,R}$ through PID controller) and the bias field term $V_{pr,R}$ which is required marginally for a minimum breakdown loop voltage. In this experiment, M and V_{fp} are left to zero for the centered as well as fixed plasma position without any bias and modulation.

Fig.4 shows as an example the plasma position displacement for both cases of flux feedback(a) and current center feedback(b). Ripple like fluctuations in the signal traces are due to the chopped voltage spikes of poloidal power supply. It can be seen that flux surface position deduced from an analysis of the full set of magnetic measurement as described in Chap.4 is essentially well controlled in flux feedback example while the position of current center shows a somewhat different behavior. The horizontal and vertical position displacements are less than 2 mm and 1 mm in steady state, respectively, which is satisfactory but the deviations from the desired position are noticeable during the start up of plasma current($t < 20$ ms in Fig.4). The difference between the flux surface position and the current center position can also be seen in the current center feedback example, Fig.4–(b). While the current center position is well centered, the flux surface position is shifted from the geometrical center of liner by more than 5 mm.

An example of isoflux surfaces on the poloidal section of these two different shots are shown in Fig.5 which is drawn by the method described in Chap.4 interchanging the position variable $\rho_{pj} = \rho_{pi} - 2 \Delta e_j$ in eq.(15). It indicates that the plasma cross section of RTP is slightly noncircular.

By introducing the flux feedback into the plasma position control, the machine performance in volt-second consumption and pulse duration is expected to be upgraded up to factor of 2 compared with that of the current center feedback method(see Fig.6). Volt-second consumption becomes larger as the plasma density goes up. The

two different shots of Fig.6 was run under the same filling pressure of 0.4 mtorr without any intermediate gas injection. Here we assume that the condition of wall recycling of hydrogen is not changed by shot.

7. Concluding Remark

Existing system controls the position of magnetic axis, while the new system controls the position of outermost magnetic flux surface. With the ex-

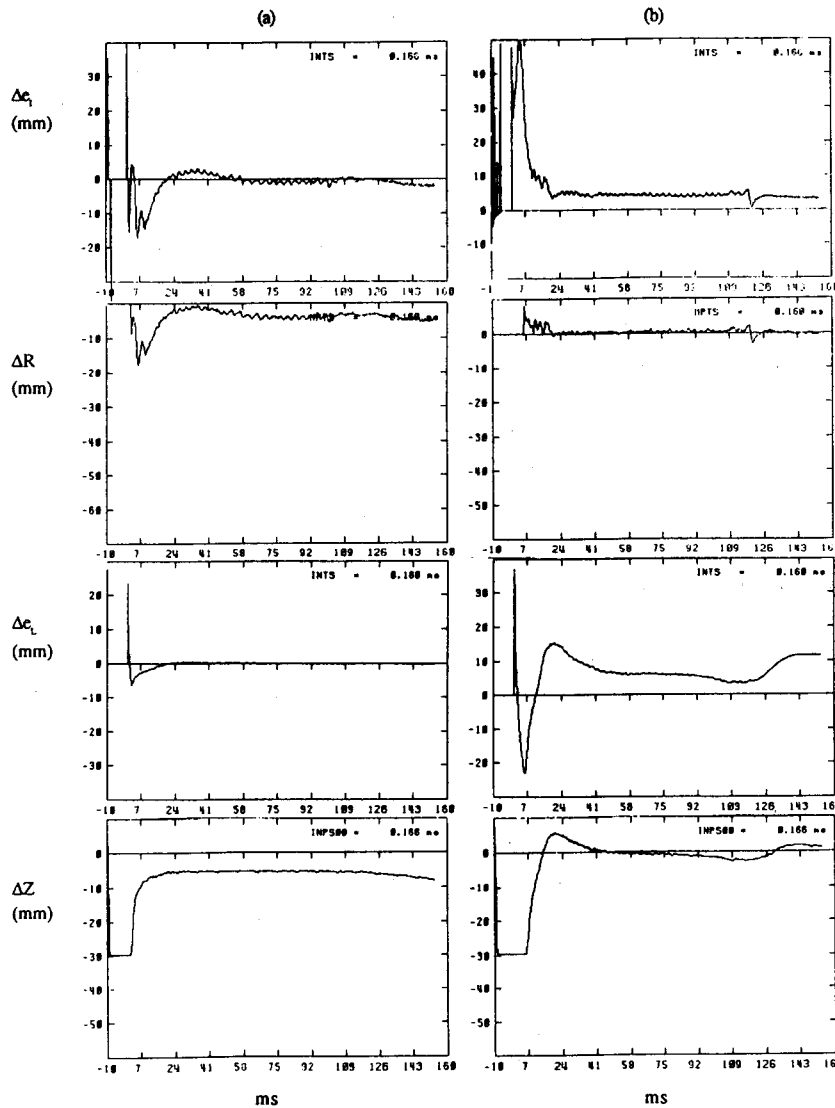


Fig. 4. Example of Plasma Position Control. Δe_1 and Δe_2 are the Flux Surface Position Displacement Variables as Defined in Chap.4 ΔR and ΔZ are the Horizontal and the Vertical Position Displacement of Current Center from the Geometrical Center of Liner. Column (a) is the Case of Flux Feedback and (b) is of Current Center Feedback.

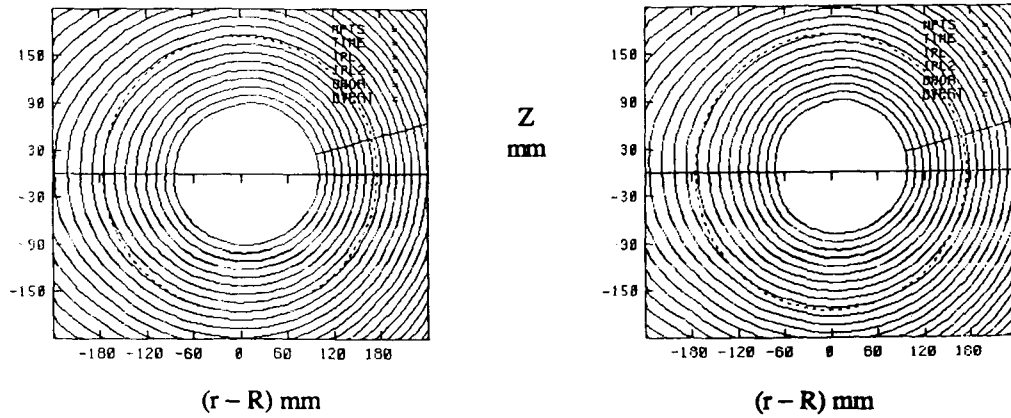


Fig. 5. An Example of Isoflux Surface on the Poloidal Cross Section. Left One is the Case of Flux Feedback [(a) of Fig. 4] and Right One is of Current Center Feedback [(b) of Fig. 4] at the Time Point of 58 ms.

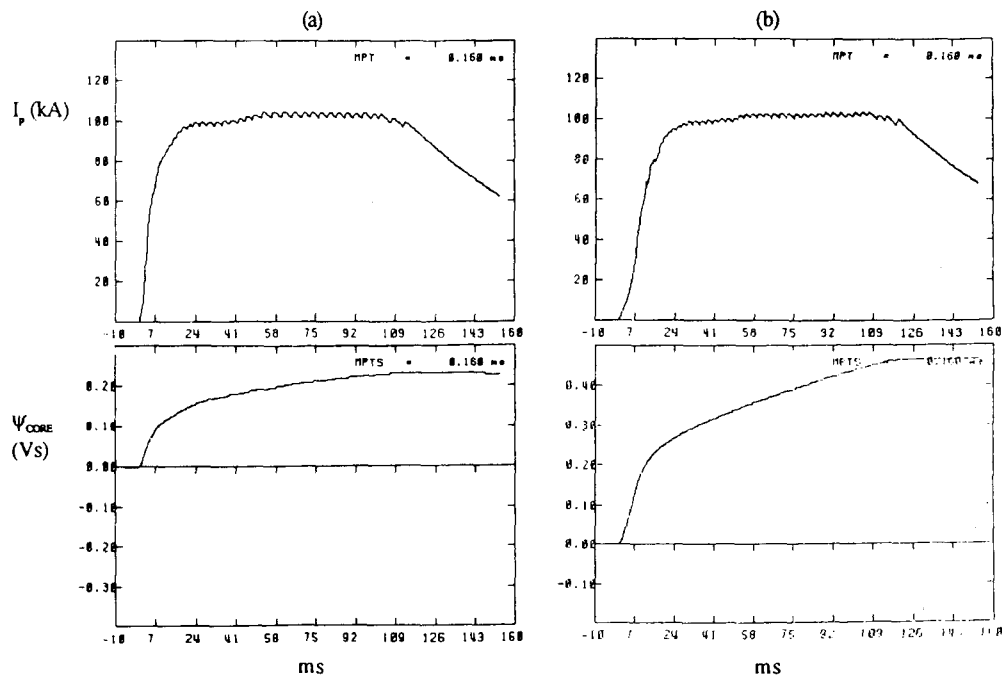


Fig. 6. Example of Performance of Position Feedback Control. (a) is the Case of Flux Feedback and (b) is of Current Center Feedback. I_p is the Plasma Current and Ψ_{CORE} is the Flux Consumption in Iron Core.

isting current center control, the breakdown and buildup of plasma current were not reliable due to the abnormally high liner current in RTP experiment. Before the onset of plasma current, flux feedback attempts to keep the average poloidal field equal to zero inside the vacuum vessel, as approximately required to obtain electrical breakdown of the filling gas. In RTP, flux feedback is applied prior to the ohmic pulse so that a highly reliable breakdown and buildup of plasma current can be achievable.

While the position control is working satisfactorily for the plasmas in normal operation mode, improvements are required to cope with the large fluctuations in position due to the heavier gas puff (see Fig.7) and ECRH power injection.

In addition to the control of the top-bottom and the inboard-outboard boundaries, it is also possible to estimate the eccentricity of the plasma cross section through some modifications in mathematical formulation of flux function, but the shape is not controllable because RTP has only two de-

grees of freedom in active coil system i.e., vertical and horizontal [6].

Plasma position control systems are all built with conventional analogue electronics and in daily use for RTP tokamak runs. Future work will concern specifying the transfer functions of power supplies and of tokamak plasma position dynamics. Digital systems based on a 68030 microprocessor are in preparation for advanced operational versatility such as the modulation of the feedback gain and the non linear feedback. For example, horizontal position drifts outward at the phase of increase of plasma density, and inward at the phase of plasma density decreasing ($\Delta e_L \sim \frac{\partial n_{line}}{\partial t}$; as shown in Fig.7). Furnishing the digital system, it is expected to have more stable and faster regulation of the plasma position during gas injection and/or the injection of ECRH power [7].

Acknowledgments

The author is grateful to Prof. F.C. Schuller and Dr. A.A.M. Oomens of the FOM-institute for plasma physics "Rijnhuizen", Nederland, for useful discussions on the plasma engineering experiments of RTP tokamak and to B. De Groot for his assistance in building electronics hardware and software support.

References

1. F.C. Schuller, The Aims of The RTP Project, Rijnhuizen ASR 1987, 19, and O.G.Kruijt et al., Proc. 15th Symposium on Fusion Technology, Utrecht, 19-23 September, 1988, 277.
2. F. Schneider, Novel Method of Determining the Plasma Position and Its Application to The ASDEX Feedback System, Proc. 10th Symposium on Fusion Technology, Padua, 4-9 September, 1978, 1013.
3. P. Noll, et al., The JET Plasma Position and

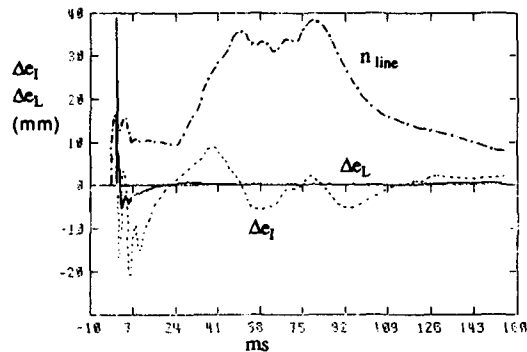


Fig. 7. Plasma Position in Gas Injection Phase. n_{line} is the Electron Line Density measured by 2 mm Interferometry. Gas Injection is Applied at the Time Point of 24 ms. During the Gas Injection, Line Density Increases more than 3 Times Than the Normal Discharge. Large Fluctuations are Shown in Horizontal Position While Vertical Position is Not Affected.

- Current Control System, Proc. 13th Symposium on Fusion Technology, Varese, 24–28 September, 1984, 503.
4. K.W. Lee, Power Crowbar System for The Pulsed DC High Magnetic Field, Korean Applied Physics, Vol.3, 1990, 466.
 5. V.S. Mukhovatov, and V.D. Shafranov, Nuclear Fusion 11, 1971, 605.
 6. K.W. Lee, et al., Feedback Control of The Plasma Position in RTP, Proc. 16th Symposium on Fusion Technology, London, 3–7 September, 1990, 1147.
 7. F.C. Shuller, et al., Experimental Observations of Ohmic and ECR Heated Tokamak Plasmas in RTP, in Controlled Fusion and Plasma Physics(Proc. 18th Eur. Conf., Berlin, 3–7 June, 1991, to be printed)